

Error-correcting codes for fermionic quantum simulation

Yu-An Chen,^{1,2,*} Alexey V. Gorshkov,¹ and Yijia Xu^{1,3,†}

¹*Joint Quantum Institute and Joint Center for Quantum Information and Computer Science,
NIST/University of Maryland, College Park, Maryland 20742, USA*

²*Condensed Matter Theory Center, University of Maryland, College Park, Maryland 20742, USA*

³*Institute for Physical Science and Technology, University of Maryland, College Park, Maryland 20742, USA*

(Dated: October 20, 2022)

We provide ways to simulate fermions by qubits on 2d lattices using \mathbb{Z}_2 gauge theories (stabilizer codes). By studying the symplectic automorphisms of the Pauli module over the Laurent polynomial ring, we develop a systematic way to increase the code distances of stabilizer codes. We identify a family of stabilizer codes that can be used to simulate fermions with code distances of $d = 2, 3, 4, 5, 6, 7$ such that any $\lfloor \frac{d-1}{2} \rfloor$ -qubit error can be corrected. In particular, we demonstrate three stabilizer codes with code distances of $d = 3$, $d = 4$, and $d = 5$, respectively, with all stabilizers and logical operators shown explicitly. The syndromes for all Pauli errors are provided. Finally, we introduce a syndrome-matching method to compute code distances numerically.

CONTENTS

I. Introduction	1
Summary of results	2
II. 2d bosonization	2
A. Review of the original bosonization	2
B. Bosonization with code distance $d = 3$	4
C. Bosonization with code distance $d = 4$	5
D. Bosonization with code distance $d = 5$	6
III. Stabilizer codes and the Pauli module	7
A. Review of the Laurent polynomial method for the Pauli algebra	7
B. New stabilizer codes developed from automorphisms	8
1. Automorphism for code distance $d = 3$	9
2. Automorphism for code distance $d = 4$	9
3. Automorphism for code distance $d = 5$	10
C. Searching algorithm for automorphisms	11
Acknowledgement	11
A. Syndrome-matching method for finding code distances	12
B. 16 elementary automorphisms	12
C. Automorphisms for code distances $d = 6$ and $d = 7$	15
References	17

I. INTRODUCTION

Error-correcting codes were originally developed to correct quantum errors on noisy quantum devices and

have found further applications in condensed matter physics and high-energy physics. The cornerstone of quantum error correction is the stabilizer formalism [1], which defines the codewords in the +1 eigenspace of an arbitrary element in an Abelian group \mathcal{G} , referred to as the stabilizer group. A stabilizer code is labeled $[[n, k, d]]$ when it uses n physical qubits to encode k logical qubits with code distance d . The code distance is the minimum weight of an operator that commutes with all elements of \mathcal{G} but is not in \mathcal{G} itself. A good stabilizer code has a high ratio $\frac{k}{n}$ and a large code distance d . In this paper, however, we address a different goal. Instead of encoding logical qubits using physical qubits, we want to encode (logical) fermions using (physical) qubits. The motivation comes from the simulation of fermions on quantum computers [2, 3]. While fault-tolerant quantum computation [4, 5] is the ultimate goal, current devices still suffer from noise, so error-mitigation schemes are crucial. Therefore, when implementing fermions with qubits, we need a design in which certain Pauli errors can be corrected directly without having to encode the underlying qubits further. Thus we want to find a systematic way to design fermion-to-qubit mappings with a large code distance d .

When a fermionic Hamiltonian consists of geometrically local terms, they can be mapped to local qubit operators by the Bravyi-Kitaev superfast encoding and its variants [2, 6], the auxiliary method [7–12], or the exact bosonization [13–18]. Variants of these mappings have been studied to minimize different cost functions. [19–21]. However, in each of these methods, extra qubits are required, i.e., the number of qubits is twice the number of fermions on the 2d square lattice. This is the price for the locality-preserving property.¹ These methods can be thought of as stabilizer codes. Given N fermions with the Hilbert space dimension 2^N , they are mapped to

* E-mail: yuanchen@umd.edu

† E-mail: yijia@umd.edu

¹ We can apply the Jordan-Wigner transformation on the 2d lattice by choosing a path including all vertices. However, some local fermionic terms will be mapped to long string operators that are highly nonlocal.

$2N$ qubits with space dimension 2^{2N} , which is an enlarged space. After N gauge constraints (stabilizer conditions) are imposed, the gauge-invariant subspace (code space) has dimension $2^{2N}/2^N = 2^N$, which matches the dimension of the fermions. It has been shown that gauge constraints can be utilized for error correction [22], and code distances can be studied for these stabilizer codes. Ref. [6] demonstrates that an improved Bravyi-Kitaev superfast encoding can correct any single-qubit error in a graph with degrees ≥ 6 . In Ref. [23], another new version of the Bravyi-Kitaev superfast encoding is proposed, called the ‘‘Majorana loop stabilizer code,’’ which is designed to have code distance $d = 3$ such that any single-qubit error can be corrected. However, these ways of encoding are very sophisticated, making it hard to generalize in order to produce larger code distances.

In this paper, we conjugate an existing stabilizer code with a Clifford circuit.² This produces a new stabilizer code. Since the new code is obtained via conjugation by a unitary operator, the algebra of the logical operators is preserved. If we choose the circuit wisely, the new stabilizer code will have a larger code distance ($d > 3$). To study Clifford circuits systematically, we utilize the Laurent polynomial method introduced in Refs. [24, 25] and further extended in Ref. [26], which shows that any Pauli operator can be written as a vector in a symplectic space. For a system with translational symmetry, i.e., the 2d square lattice, the space of Pauli operators becomes a module over a polynomial ring. Further, this polynomial method can be used to formulate 2d bosonization concisely [27]. The commutation relations of Pauli operators are determined by the symplectic form. Ref. [28] shows that there is a one-to-one correspondence (up to a translation operator on the lattice):

$$\begin{aligned} &\text{Automorphism of the symplectic form} \\ \iff &\text{Clifford circuit on a 2d square lattice.} \end{aligned}$$

Therefore, the problem becomes searching for ‘‘good’’ automorphisms of the Pauli module with the symplectic form, which can be achieved efficiently by numerical enumerations.

Summary of results

In this work, we use the Laurent polynomial method to construct bosonizations on a 2d square lattice. Table I is the summary of our results. In Section II, we review the original 2d bosonization method [13] in Ref. II A and then pictorially construct 2d bosonizations with a distance of 3, 4, and 5 in Sections II B, II C, and II D, respectively.

We review the Laurent polynomial method in Section III A. In Sections III B 1, III B 2, and III B 3, we

describe all these bosonizations within the framework of the Laurent polynomial method. In addition, we describe a computerized method to automatically search bosonizations in Section III C.

In Appendix A, we discuss the ‘‘syndrome matching’’ method used to compute the code distance of a given bosonization. In Appendix B, we describe 16 elementary automorphisms. In Appendix C, we show the polynomial representations of an automorphism with a distance of 6 and another with a distance of 7.

II. 2D BOSONIZATION

In Section II A, we begin by reviewing the original 2d bosonization on a square lattice from Ref. [13]. Then, we demonstrate a new way to perform bosonization with a code distance of $d = 3$, $d = 4$, and $d = 5$ in Section II B, Section II C, and Section II D, respectively.

A. Review of the original bosonization

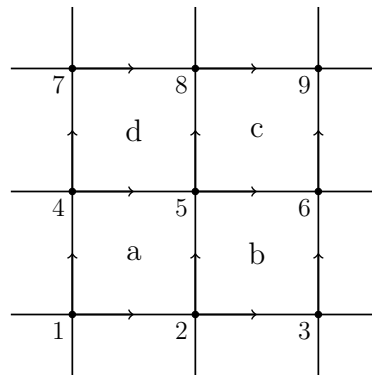


FIG. 1. Bosonization on a square lattice [13]. We put Pauli matrices X_e , Y_e , and Z_e on each edge and one complex fermion c_f, c_f^\dagger on each face. We will work in the Majorana basis $\gamma_f = c_f + c_f^\dagger$ and $\gamma'_f = -i(c_f - c_f^\dagger)$ for convenience.

We first describe the Hilbert space in Fig. 1. The elements associated with vertices, edges, and faces will be denoted by v , e , and f , respectively. On each face f of the lattice, we place a single pair of fermionic creation-annihilation operators c_f, c_f^\dagger , or equivalently a pair of Majorana fermions γ_f, γ'_f . The even fermionic algebra consists of local observables with a trivial fermionic parity, i.e., local observables that commute with the total fermion parity $(-1)^F \equiv \prod_f (-1)^{c_f^\dagger c_f}$.³ The even algebra is generated by [13]:

² A circuit U is Clifford if and only if UPU^\dagger is a product of Pauli matrices for any given Pauli matrix P .

³ The even fermionic algebra can also be considered as the algebra of local observables containing an even number of Majorana operators.

	distance	occupation	hopping	density-density	stabilizer
Bravyi-Kitaev superfast encoding	2	4	6	6	6
Majorana loop stabilizer code	3	3	3-4	4-6	4-10
Exact bosonization ($d = 3$)	3	4	3-5	6	8
Exact bosonization ($d = 4$)	4	6	5-6	10	10
Exact bosonization ($d = 5$)	5	8	5-9	12-14	12
Exact bosonization ($d = 6$)	6	12	6-13	16-20	18
Exact bosonization ($d = 7$)	7	12	7-23	16-18	26

TABLE I. A comparison of codes based on modified exact bosonization to the Bravyi-Kitaev superfast encoding [2] and the Majorana loop stabilizer code [23] on a 2d square lattice. The $d = 2$ exact bosonization is equivalent to the Bravyi-Kitaev superfast encoding with a specific choice of the ordering of edges [21]. We list the code distance, as well as the weights (after mapping to qubits) of a fermion occupation term (local fermion parity term), of a hopping term, and of a density-density interaction between nearest neighbors. The weights of the stabilizers are also shown.

1. On-site fermion parity:

$$P_f \equiv -i\gamma_f\gamma'_f. \quad (1)$$

2. Fermionic hopping term:

$$S_e \equiv i\gamma_{L(e)}\gamma'_{R(e)}, \quad (2)$$

where $L(e)$ and $R(e)$ are faces to the left and right of e , with respect to the orientation of e in Fig. 1.

The bosonic dual of this system involves \mathbb{Z}_2 -valued spins on the edges of the square lattice. For every edge e , we define a unitary operator U_e that squares to 1. Labeling the faces and vertices as in Fig. 1, we define:

$$\begin{aligned} U_{56} &= X_{56}Z_{25}, \\ U_{58} &= X_{58}Z_{45}, \end{aligned} \quad (3)$$

where X_e, Z_e are Pauli matrices acting on a spin at each edge e :

$$X_e = \begin{bmatrix} 0 & 1 \\ 1 & 0 \end{bmatrix}, \quad Z_e = \begin{bmatrix} 1 & 0 \\ 0 & -1 \end{bmatrix}. \quad (4)$$

Operators U_e for the other edges are defined by using translation symmetry. Pictorially, operator U_e is depicted as

$$U_e = \begin{array}{c} | \\ X_e \\ -Z- \end{array} \quad \text{or} \quad \begin{array}{c} -X_e- \\ | \\ Z \end{array}, \quad (5)$$

corresponding to the vertical or horizontal edge e .

In Ref. [13], U_e and S_e are shown to satisfy the same commutation relations. We also map the fermion parity

P_f at each face f to the ‘‘flux operator’’ $W_f \equiv \prod_{e \subset f} Z_e$, the product of Z_e around a face f :

$$W_f = \begin{array}{c} -Z- \\ | \\ Z \quad f \quad Z \\ | \\ -Z- \end{array}. \quad (6)$$

The bosonization map is

$$\begin{aligned} S_e &\longleftrightarrow U_e, \\ P_f &\longleftrightarrow W_f, \end{aligned} \quad (7)$$

or pictorially

$$\begin{aligned} i \times \begin{array}{c} \gamma_{L(e)} \\ e \\ \gamma'_{R(e)} \end{array} &\longleftrightarrow \begin{array}{c} -X_e- \\ | \\ Z \end{array}, \\ i \times \begin{array}{c} \gamma_{L(e)} \\ | \\ e \quad \gamma'_{R(e)} \end{array} &\longleftrightarrow \begin{array}{c} | \\ X_e \\ -Z- \end{array}, \end{aligned} \quad (8)$$

$$-i\gamma_f\gamma'_f \longleftrightarrow \begin{array}{c} -Z- \\ | \\ Z \quad f \quad Z \\ | \\ -Z- \end{array}.$$

The condition $P_a P_c S_{58} S_{56} S_{25} S_{45} = 1$ on fermionic operators gives a gauge (stabilizer) constraint $G_v =$

⁴ $P_f = -i\gamma_f\gamma'_f = (-1)^{c_f c_f}$ measures the occupancy of the fermion at face f .

$W_{f_c} \prod_{e \supset v_5} X_e = 1$ for bosonic operators, or generally

$$G_v = \begin{array}{c} \text{---}Z\text{---} \\ | \quad | \\ XZ \quad Z \\ | \quad | \\ \text{---}X\text{---}v\text{---}XZ\text{---} \\ | \\ X \\ | \end{array} = 1. \quad (9)$$

The gauge constraint Eq. (9) can be considered as the stabilizer ($G_v |\Psi\rangle = |\Psi\rangle$ for $|\Psi\rangle$ in the code space), which forms the stabilizer group \mathcal{G} . The operators U_e and W_f generate all logical operators.⁵ The weight of a Pauli string operator O is the number of Pauli matrices in O , denoted as $\text{wt}(O)$. For example, we have $\text{wt}(U_{56}) = \text{wt}(U_{58}) = 2$ and $\text{wt}(W_f) = 4$. The code distance d is defined as the minimum weight of a logical operator excluding stabilizers:

$$d = \min\{\text{wt}(O) \mid [O, \mathcal{G}] = 0, O \notin \mathcal{G}\}. \quad (10)$$

The code distance of this original bosonization is $d = 2$ as U_e has weight 2 and any single Pauli matrix violates at least one G_v , which implies that there is no logical operator with weight 1.

There are 4 types of nearest-neighbor hopping terms ($\gamma_L \gamma'_R$, $\gamma_L \gamma_R$, $\gamma'_L \gamma'_R$, and $\gamma'_L \gamma_R$) and one type of fermion occupation term ($-i\gamma_f \gamma'_f$). When mapped to Pauli matrices, their weights wt_i are in the range $2 \leq \text{wt}_i \leq 6$. The maximum weight corresponds to the worst case to simulate the fermion hopping term or the fermion occupation term. A good stabilizer code requires a balance between the minimum weight and the maximum weight. A high minimum weight guarantees the error-correcting property, while a low maximum weight implies that the cost of simulation is low. We label the minimum and maximum weights of the hopping terms as wt_{\min} and wt_{\max} . In this example, $(\text{wt}_{\min}, \text{wt}_{\max}) = (2, 6)$.

B. Bosonization with code distance $d = 3$

We now introduce a new way to map the fermionic operators S_e and P_f to Pauli matrices. For simplicity, we present the mapping in a pictorial way:

$$i \times \frac{\gamma_{L(e)}}{e} \longleftrightarrow \begin{array}{c} | \\ Z \\ | \\ \text{---}X_e\text{---} \\ | \\ Z \\ | \end{array}, \quad (11)$$

$$i \times \left. \begin{array}{c} \gamma_{L(e)} \\ | \\ e \\ | \\ \gamma'_{R(e)} \end{array} \right\} \longleftrightarrow \begin{array}{c} | \\ X_e \\ | \\ \text{---}Z\text{---} \quad \text{---}Z\text{---} \\ | \end{array},$$

$$-i\gamma_f \gamma'_f \longleftrightarrow \begin{array}{c} \text{---}Z\text{---} \\ | \quad | \\ Z \quad f \quad Z \\ | \quad | \\ \text{---}Z\text{---} \end{array}.$$

The stabilizer on the bosonic side is

$$G_v^{d=3} = (-1) \times \begin{array}{c} \text{---}Z\text{---} \\ | \quad | \\ Z \quad X \quad Z \\ | \quad | \\ \text{---}X\text{---}v\text{---}X\text{---} \\ | \\ X \\ | \\ \text{---}Z\text{---} \end{array} = 1. \quad (12)$$

Notice that there is a minus sign coming from $ZXZ = -X$.⁶ We can manually check that the logical operators defined in Eq. (11) do commute with the stabilizer in Eq. (12). We will prove that this mapping preserves the fermionic algebra in the next section.

Given the stabilizer, we can provide the syndromes for all the single-qubit Pauli errors, as shown in Fig. 2. We see that all single-qubit Pauli matrices have different syndromes, which means that we do not have any logical operators with weight 2. This implies a code distance of $d \geq 3$. Eq. (11) shows logical operators with weight 3, so we conclude that the code distance is $d = 3$. Based on the syndrome measurements, we can always correct any single-qubit error according to Fig. 2.

The 4 types of nearest-neighbor hopping terms, $\gamma_L \gamma'_R$, $\gamma_L \gamma_R$, $\gamma'_L \gamma'_R$, and $\gamma'_L \gamma_R$ have weights wt_i in the range $3 \leq \text{wt}_i \leq 5$. Therefore, the modified bosonization has $(\text{wt}_{\min}, \text{wt}_{\max}) = (3, 5)$ and a fermionic occupation term of weight 4. Compared to the original bosonization with $(\text{wt}_{\min}, \text{wt}_{\max}) = (2, 6)$, the minimum weight is increased such that error-correction can be performed, while the maximum weight of the hopping terms is decreased implying a reduction in the simulation cost.

⁵ The logical operators consist of all operators that commute with \mathcal{G} . \mathcal{G} are trivial logical operators as stabilizers have no effect on the code space. U_e and W_f together generate all the other logical operators.

⁶ The stabilizer is derived from the identity $P_a P_c S_{58} S_{56} S_{25} S_{45} = 1$. After we map P_f and S_e to the Pauli matrices using Eq. (11), it becomes $G_v^{d=3}$.

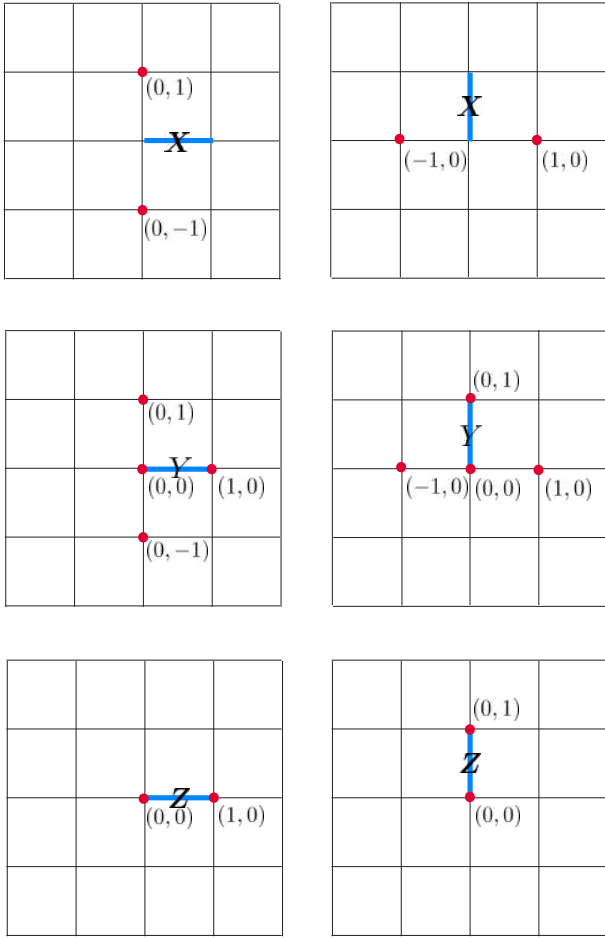


FIG. 2. Syndromes of single-qubit errors for the bosonization with code distance $d = 3$. The red vertices v represent locations where the single-qubit error does not commute with the stabilizer G_v .

C. Bosonization with code distance $d = 4$

In this section, we provide a construction of an exact bosonization with code distance $d = 4$ as an intermediate step toward $d = 5$. Since its code distance is $d = 4$, which is even, this code (like the $d = 3$ code) can only correct $\lfloor \frac{d-1}{2} \rfloor = 1$ Pauli error. However, for error deflection, Pauli errors up to weight 3 can be observed from the syndrome measurements of the stabilizers.

The mapping can be described as

$$\begin{aligned}
 i \times \frac{\gamma_{L(e)}}{\gamma'_{R(e)}} e &\leftrightarrow \begin{array}{c} -X_e- \\ | \\ Z \\ | \\ -X- \\ | \\ Z \end{array}, \\
 i \times \gamma_{L(e)} \left| e \right. \gamma'_{R(e)} &\leftrightarrow \begin{array}{c} -Z- \quad -Z- \\ | \quad | \\ X \quad X_e \\ | \quad | \\ -Z- \end{array}, \\
 -i\gamma_f \gamma'_f &\leftrightarrow \begin{array}{c} -Z- \\ | \\ X \quad f \\ | \quad | \\ -XZ- \quad -X- \\ | \quad | \\ XZ \quad Z \end{array}.
 \end{aligned} \tag{13}$$

The stabilizer becomes

$$G_v^{d=4} = \begin{array}{c} -Z- \\ | \\ X \\ | \quad -Z- \\ | \quad | \\ Z \quad Z \\ | \quad | \\ -XZ- \quad v \quad -Z- \quad -X- \\ | \quad | \\ XZ \quad Z \end{array} = 1. \tag{14}$$

We can check that the logical operators in Eq. (13) commute with the stabilizer in Eq. (14). The proof for the equivalence between the even fermionic algebra and this stabilizer code will be shown in the next section.

The syndromes for all single-qubit Pauli errors are provided in Fig. 3. From the generators of the logical operators in Eq. (13), we may be tempted to conclude that the code distance is $d = 5$ because the minimum weight is 5. However, based on the syndromes in Fig. 3, we find

that $d = 5$. This code has an error-correcting property for any two-qubit error.

We show that any two-qubit error has a unique syndrome and, therefore, that the code distance is $d = 5$. In conclusion, we provide a way to simulate fermions by qubits on the 2d square lattice, such that any two-qubit Pauli error can be corrected.

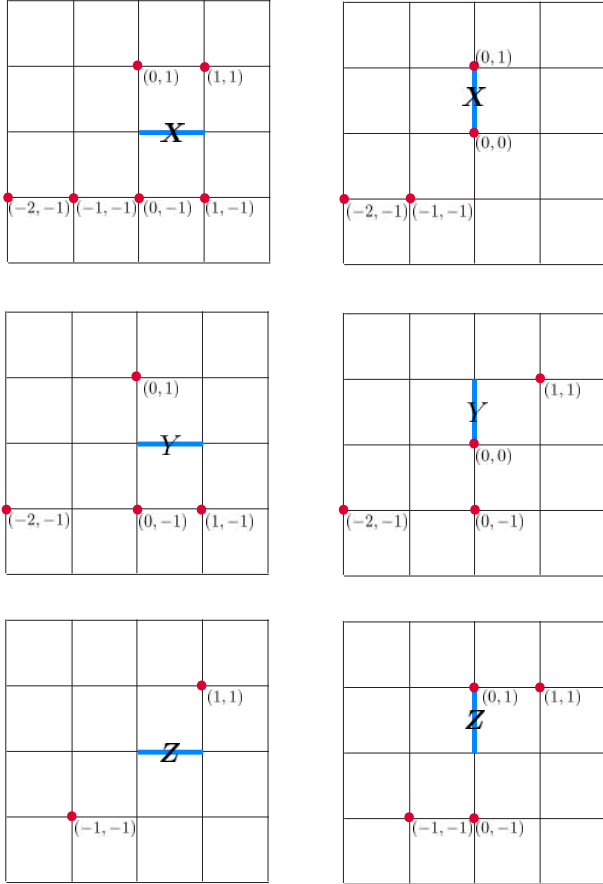


FIG. 4. Syndromes of single-qubit errors for the $d = 5$ bosonization.

III. STABILIZER CODES AND THE PAULI MODULE

In this section, we first review the Laurent polynomial method in Section III A. Then, in Section III B, we discuss bosonization with distance $d = 3, 4, 5$ and the corresponding symplectic automorphisms. The searching algorithm for automorphisms is presented in Section III C.

A. Review of the Laurent polynomial method for the Pauli algebra

We review the polynomial expression for any Pauli operator by a vector over a polynomial ring $R =$

$\mathbb{F}_2[x, y, x^{-1}, y^{-1}]^7$ as set out in Ref. [24]. First, we define X_{12} , Z_{12} , X_{14} , and Z_{14} in Fig. 1 as column vectors:

$$X_{12} = \begin{bmatrix} 1 \\ 0 \\ 0 \\ 0 \end{bmatrix}, \quad Z_{12} = \begin{bmatrix} 0 \\ 0 \\ 1 \\ 0 \end{bmatrix}, \quad X_{14} = \begin{bmatrix} 0 \\ 1 \\ 0 \\ 0 \end{bmatrix}, \quad Z_{14} = \begin{bmatrix} 0 \\ 0 \\ 0 \\ 1 \end{bmatrix}. \quad (20)$$

All the other edges can be defined with the help of translation operators as follows. We use polynomials of x and y to represent translation in the x and y directions, respectively. For example,

$$Z_{78} = y^2 \begin{bmatrix} 0 \\ 0 \\ 1 \\ 0 \end{bmatrix} = \begin{bmatrix} 0 \\ 0 \\ y^2 \\ 0 \end{bmatrix}, \quad X_{58} = xy \begin{bmatrix} 0 \\ 1 \\ 0 \\ 0 \end{bmatrix} = \begin{bmatrix} 0 \\ xy \\ 0 \\ 0 \end{bmatrix}. \quad (21)$$

More examples are included in Fig. 5.

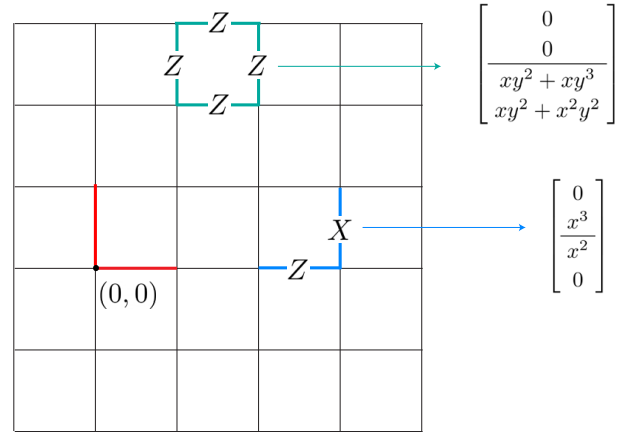


FIG. 5. Examples of polynomial expressions for Pauli strings. The flux term (i.e. fermionic occupation) on a plaquette and the hopping term on an edge are both shown. The factors such as x^2y^2 and x^2 represent the locations of the operators relative to the origin.

To determine whether two Pauli operators represented by vectors v_1 and v_2 commute or anti-commute, we defining the dot product as

$$v_1 \cdot v_2 = \bar{v}_1 \Lambda v_2, \quad (22)$$

where $\bar{\cdot}$ is the transpose operation on a matrix along

⁷ This is the ring that consists of all polynomials of x, x^{-1}, y, y^{-1} with coefficients in \mathbb{F}_2 .

with $x, y \rightarrow x^{-1}, y^{-1}$ and

$$\Lambda = \left[\begin{array}{cc|cc} 0 & 0 & 1 & 0 \\ 0 & 0 & 0 & 1 \\ \hline -1 & 0 & 0 & 0 \\ 0 & -1 & 0 & 0 \end{array} \right]. \quad (23)$$

Notice that -1 is the same as 1 here because we are working on the \mathbb{Z}_2 field. The minus sign just reminds us of the symplectic form. The two operators v_1 and v_2 commute if and only if the constant term of $v_1 \cdot v_2$ is zero. For example, we calculate the dot products

$$X_{12} \cdot Z_{12} = 1, \quad X_{58} \cdot Z_{14} = x^{-1}y^{-1}, \quad (24)$$

and, therefore, X_{12} and Z_{12} anti-commute, whereas X_{58} and Z_{14} commute (their dot product only has a non-constant term $x^{-1}y^{-1}$). Furthermore, $X_{58} \cdot Z_{14} = x^{-1}y^{-1}$ means that the shifting of X_{58} in $-x$ and $-y$ directions by 1 step, respectively, will anti-commute with Z_{14} . This dot product defined by Λ is referred to as the symplectic form. A translationally invariant stabilizer code forms an R -submodule⁸ V such that

$$v_1 \cdot v_2 = \bar{v}_1 \Lambda v_2 = 0, \quad \forall v_1, v_2 \in V. \quad (25)$$

We now study the automorphisms A of the symplectic form Λ :

$$(Av_1) \cdot (Av_2) = v_1 \cdot v_2, \quad \forall v_1, v_2 \in V. \quad (26)$$

This is equivalent to $\bar{A}\Lambda A = \Lambda$, which, taking $A = \left[\begin{array}{cc|cc} a & b & & \\ c & d & & \end{array} \right]$, becomes

$$\left[\begin{array}{cc|cc} \bar{a} & \bar{c} & & \\ \bar{b} & \bar{d} & & \end{array} \right] \left[\begin{array}{cc|cc} 0 & I & & \\ -I & 0 & & \end{array} \right] \left[\begin{array}{cc|cc} a & b & & \\ c & d & & \end{array} \right] = \left[\begin{array}{cc|cc} 0 & I & & \\ -I & 0 & & \end{array} \right] \quad (27)$$

$$\Rightarrow \bar{a}d - \bar{c}b = I, \quad \bar{a}c = \bar{c}a, \quad \bar{b}d = \bar{d}b.$$

Examples of the automorphism A are

$$\begin{aligned} S &= \left[\begin{array}{cc|cc} I & 0 & & \\ c & I & & \end{array} \right], \text{ where } c \in \text{Mat}_2[R] \text{ and } \bar{c} = c, \\ H &= \left[\begin{array}{cc|cc} 0 & I & & \\ -I & 0 & & \end{array} \right], \\ C &= \left[\begin{array}{cc|cc} 1 & 0 & 0 & 0 \\ r & 1 & 0 & 0 \\ \hline 0 & 0 & 1 & \bar{r} \\ 0 & 0 & 0 & 1 \end{array} \right], \text{ where } r \in R. \end{aligned} \quad (28)$$

$\text{Mat}_2[R]$ consists of all 2×2 matrices with entries in $R = \mathbb{F}_2[x, y, x^{-1}, y^{-1}]$.

B. New stabilizer codes developed from automorphisms

First, we reformulate the original bosonization introduced in Section II A and incorporate it into the Pauli module. For simplicity, we will write x^{-1} and y^{-1} as \bar{x} and \bar{y} , respectively. The original hopping operators U_e in Eq. (5) can be written as

$$U_1 = \left[\begin{array}{c} 1 \\ 0 \\ 0 \\ \bar{y} \end{array} \right], \quad U_2 = \left[\begin{array}{c} 0 \\ 1 \\ \bar{x} \\ 0 \end{array} \right], \quad (29)$$

where U_1 represents U_e on the horizontal edge and U_2 represents U_e on the vertical edge. The flux term W_f in (6) is written as

$$W = \left[\begin{array}{c} 0 \\ 0 \\ 1+y \\ 1+x \end{array} \right]. \quad (30)$$

The stabilizer G_v in Eq. (9) corresponds to the vector

$$G = \left[\begin{array}{c} 1+\bar{x} \\ 1+\bar{y} \\ 1+y \\ 1+x \end{array} \right]. \quad (31)$$

Now, we will apply automorphisms on these vectors to generate new stabilizer codes.

⁸ The R -submodule is similar to a subspace of a vector space, but the entries of the vector are in the ring $R = \mathbb{F}_2[x, y, x^{-1}, y^{-1}]$. In a ring, the inverse element may not exist. This is the distinction between a module and a vector space.

1. Automorphism for code distance $d = 3$

We consider the simplest automorphism

$$A_1 = \left[\begin{array}{cc|cc} 1 & 0 & 0 & 0 \\ 0 & 1 & 0 & 0 \\ \hline 0 & 1 & 1 & 0 \\ 1 & 0 & 0 & 1 \end{array} \right], \quad (32)$$

which modifies the Pauli operator X_e as

$$A_1 \begin{bmatrix} 1 \\ 0 \\ 0 \\ 0 \end{bmatrix} = \begin{bmatrix} 1 \\ 0 \\ 0 \\ 1 \end{bmatrix}, \quad A_1 \begin{bmatrix} 0 \\ 1 \\ 0 \\ 0 \end{bmatrix} = \begin{bmatrix} 0 \\ 1 \\ 1 \\ 0 \end{bmatrix}. \quad (33)$$

Pictorially, this is equivalent to

$$X_e = \begin{cases} -X_e- & \xrightarrow{A_1} \begin{array}{c} | \\ Z \\ -X_e- \end{array} \\ \begin{array}{c} | \\ X_e \end{array} & \xrightarrow{A_1} \begin{array}{c} | \\ X_e \\ -Z- \end{array} \end{cases}. \quad (34)$$

Notice that Z_e is unchanged under this automorphism. This automorphism corresponds to the Clifford circuit shown in Fig. 6.

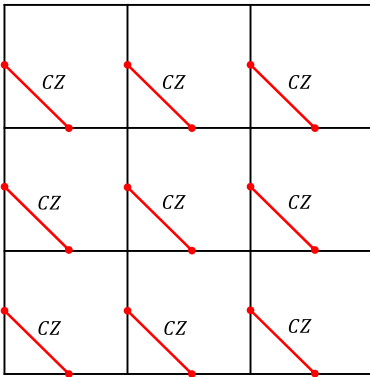


FIG. 6. Clifford circuit corresponds to automorphism A_1

Now, we apply A_1 on the logical operators U_1, U_2 , and W and the stabilizer G :

$$A_1 U_1 = \begin{bmatrix} 1 \\ 0 \\ 0 \\ 1 + \bar{y} \end{bmatrix}, \quad A_1 U_2 = \begin{bmatrix} 0 \\ 1 \\ 1 + \bar{x} \\ 0 \end{bmatrix}, \quad (35)$$

$$A_1 W = \begin{bmatrix} 0 \\ 0 \\ 1 + y \\ 1 + x \end{bmatrix}, \quad A_1 G = \begin{bmatrix} 1 + \bar{x} \\ 1 + \bar{y} \\ y + \bar{y} \\ x + \bar{x} \end{bmatrix}.$$

The automorphism A_1 applied on U_e can be visualized as

$$U_e = \begin{cases} \begin{array}{c} | \\ X_e \\ -Z- \end{array} & \xrightarrow{A_1} & \begin{array}{c} | \\ X_e \\ -Z- \end{array} \\ \begin{array}{c} | \\ -X_e- \\ Z \end{array} & \xrightarrow{A_1} & \begin{array}{c} | \\ Z \\ -X_e- \\ Z \end{array} \end{cases}. \quad (36)$$

The flux term Eq. (6) is unchanged. The automorphism A_1 applied on the stabilizer G_v is

$$\begin{array}{c} -Z- \\ | \\ XZ \\ -X-v-XZ- \\ | \\ X \end{array} \xrightarrow{A_1} \begin{array}{c} -Z- \\ | \\ Z \\ -X-v-X- \\ | \\ X \\ -Z- \end{array}. \quad (37)$$

This is the bosonization with code distance $d = 3$ introduced in Section II B. As we only apply the automorphism of the Pauli module on the original bosonization, the logical operators satisfy the same algebra. Therefore, we conclude that this new stabilizer code is a valid way to simulate fermions.

2. Automorphism for code distance $d = 4$

In this part, we consider a slightly more complicated automorphism A' 9:

$$A' = \left[\begin{array}{cc|cc} 1 & 0 & 0 & 1 \\ 0 & 1 & 1 & 0 \\ \hline 0 & \bar{x}y & 1 + \bar{x}y & 0 \\ x\bar{y} & 0 & 0 & 1 + x\bar{y} \end{array} \right]. \quad (38)$$

One can easily check that A' indeed satisfies condition Eq. (27) for being an automorphism. Applying A' on the logical operators U_1, U_2 , and W and the stabilizer

⁹ $A' = A_4 A_7$ in terms of the elementary automorphisms defined in Appendix B.

G , we get

$$\begin{aligned}
 A'U_1 &= \begin{bmatrix} 1 + \bar{y} \\ 0 \\ 0 \\ x\bar{y}^2 + x\bar{y} + \bar{y} \end{bmatrix}, \\
 A'U_2 &= \begin{bmatrix} 0 \\ 1 + \bar{x} \\ \bar{x} + \bar{x}y + \bar{x}^2y \\ 0 \end{bmatrix}, \\
 A'W &= \begin{bmatrix} 1 + x \\ 1 + y \\ 1 + y + \bar{x} + \bar{x}y^2 \\ 1 + x + \bar{y} + \bar{y}x^2 \end{bmatrix}, \\
 A'G &= \begin{bmatrix} x + \bar{x} \\ y + \bar{y} \\ 1 + y + \bar{x} + \bar{x}y^2 \\ 1 + x + \bar{y} + \bar{y}x^2 \end{bmatrix}.
 \end{aligned} \tag{39}$$

The operators $A'(U_e)$ can be depicted as

$$U_e = \left\{ \begin{array}{l} \begin{array}{c} X_e \\ | \\ -Z- \\ | \\ -X_e- \\ | \\ Z \end{array} \xrightarrow{A'} \begin{array}{c} -Z- \quad -Z- \\ | \quad | \\ X \quad X_e \\ | \quad | \\ -Z- \\ | \\ -X_e- \\ | \\ Z \end{array} \\ \\ \begin{array}{c} -X_e- \\ | \\ Z \end{array} \xrightarrow{A'} \begin{array}{c} -X_e- \\ | \\ Z \quad Z \\ | \quad | \\ -X- \\ | \\ Z \end{array} \end{array} \right. \tag{40}$$

The stabilizer $A'(G_v)$ is

$$\begin{array}{c} \begin{array}{c} -Z- \\ | \\ XZ \\ | \quad | \\ -X- v -XZ- \\ | \\ X \end{array} \xrightarrow{A'} \begin{array}{c} -Z- \\ | \\ X \\ | \quad | \\ -Z- \\ | \quad | \\ Z \quad Z \\ | \quad | \\ -Y- v -Z- -X- \\ | \\ Y \end{array} \end{array} \tag{41}$$

The logical operator U_e and the stabilizer G_v are mapped on the bosonization with code distance $d = 4$ in Section II C.

comes

$$W_f = \begin{array}{c} \begin{array}{c} -Z- \\ | \\ Z \quad f \quad Z \\ | \\ -Z- \end{array} \xrightarrow{A'} \begin{array}{c} -Z- \\ | \\ X \\ | \quad | \\ -Z- \quad -Z- \\ | \quad | \\ Y \quad f \quad Z \\ | \quad | \\ v -Y- \quad -X- \\ | \quad | \\ Z \quad Z \end{array} \end{array} \tag{42}$$

This term can be simplified by multiplying it by $A'(G_v)$, which does not change the effective logical operation. The resulting flux term is

$$\begin{array}{c} \begin{array}{c} -Z- \\ | \\ X \quad f \\ | \quad | \\ -Y- \quad -X- \\ | \quad | \\ Y \quad Z \end{array} \end{array}, \tag{43}$$

which matches Eq. (13) in Section II C.

3. Automorphism for code distance $d = 5$

We introduce another automorphism A'' ¹⁰:

$$A'' = \left[\begin{array}{cc|cc} 1 & \bar{x} & x & 1 \\ 1 & \bar{x} + 1 & 1 + x & 1 \\ \hline x & \bar{x} + 1 & \bar{x} + 1 + x + x^2 & 1 + x \\ x & 1 & x + x^2 & 1 + x \end{array} \right]. \tag{44}$$

Again it is easy to check that it satisfies condition Eq. (27) for being an automorphism. Applying A'' on the logical operators U_1 , U_2 , and W and the stabilizer

Finally, the flux term under the automorphism A' be-

¹⁰ $A'' = A_9 A_3 A_7 A_{14}$ in terms of the elementary automorphisms defined in Appendix B.

G , we get

$$A''U_1 = \begin{bmatrix} 1 + \bar{y} \\ 1 + \bar{y} \\ \bar{y} + x\bar{y} + x \\ \bar{y} + x\bar{y} + x \end{bmatrix}, \quad (45)$$

$$A''U_2 = \begin{bmatrix} 1 + \bar{x} \\ 0 \\ \bar{x}^2 + x \\ x \end{bmatrix}, \quad (46)$$

$$A''(W + G) = \begin{bmatrix} \bar{x}\bar{y} + 1 \\ \bar{x}\bar{y} + \bar{y} \\ \bar{x}\bar{y} + \bar{y} + \bar{x} + x \\ \bar{y} + x \end{bmatrix}, \quad (47)$$

$$A''G = \begin{bmatrix} \bar{x}\bar{y} + xy \\ \bar{x}\bar{y} + \bar{y} + y + xy \\ \bar{x}\bar{y} + \bar{y} + \bar{x}y + y + xy + x^2y \\ \bar{y} + 1 + xy + x^2y \end{bmatrix}. \quad (48)$$

The $A'(U_e)$ operators can be depicted as Eq. (16) and (17). Here, we choose $A''(W + G)$ as our flux operator shown in Eq. (18) because it has a lower weight $\text{wt}[A''(W + G)] < \text{wt}(A''W)$. The pictorial representation of stabilizer $A''G$ is Eq. (19).

C. Searching algorithm for automorphisms

In this subsection, we describe how we find automorphisms with code distances $d = 3, 4, 5, 6$, and 7 . The automorphisms A_1 in Eq. (32), A' in Eq. (38), and A'' in Eq. (44) correspond to the examples for $d = 3$, $d = 4$, and $d = 5$, respectively. We will show other examples with different code distances.

First, we consider 16 elementary automorphisms A_1, A_2, \dots, A_{16} (shown in Appendix B), which attach no more than one new Pauli matrix to the original Pauli matrix. For example, the A_1 automorphism attaches one Z to X_e , as shown in Eq. (33). Given the 16 elementary automorphisms, their product $A_{i_1}A_{i_2}A_{i_3}A_{i_4}\dots$ with $i_n \in \{1, 2, \dots, 16\}$ is also an automorphism. (We note that these elementary automorphisms do not generate all automorphisms.) We find that the product of five elementary automorphisms $A_{i_1}A_{i_2}A_{i_3}A_{i_4}A_{i_5}$ are sufficient to generate the code distance $d = 7$; therefore, we focus on products with five or fewer elementary automorphisms. We now describe how we search for automorphisms with large code distances:

1. We write down the bosonization of all the nearest-neighbor and on-site terms generated by S_e and P_f . They include the automorphism acting on $U_1, U_2, W, U_1 + W, U_1 + \bar{y}W, U_1 + \bar{y}W + W, U_2 + W,$

$$U_2 + \bar{x}W, U_2 + \bar{x}W + W.^{11}$$

2. We use the minimum weight of bosonization of nearest-neighbor hopping terms to roughly estimate the code distance of a given bosonization (automorphism) A .
3. We choose some candidate automorphisms with an appropriate minimum weight d , to find a bosonization with desired code distance d .
4. We apply the syndrome matching method shown in Appendix A to the candidate automorphisms. By applying syndrome matching, we find a lower bound of their code distances.
5. We apply the syndrome matching method for distance $d + 1$ to an automorphism \tilde{A} with a lower bound d . If syndrome matching for distance $d + 1$ returns a logical operators with no syndrome, we conclude that \tilde{A} is a bosonization with code distance d .

Applying the syndrome-matching method, we found automorphisms to generate exact bosonization with $d = 3, 4, 5, 6, 7$ (see Table II).

Code distance	Automorphisms
3	A_1 (3,5)
4	A_4A_7 (5,6), $A_2A_7A_1$ (4,6)
5	$A_9A_3A_7A_{14}$ (5,9)
6	$A_1A_5A_{14}A_1$ (6, 13), $A_4A_9A_{16}A_{11}$ (7, 17)
7	$A_1A_{11}A_5A_{14}A_9$ (7, 23)

TABLE II. The possible automorphisms for different code distances. The numbers inside the parentheses are the minimum and maximum weights of the logical operators for the nearest-neighbor terms. For example, $A_9A_3A_7A_{14}$ has the minimum logical weight 5 and the maximum logical weight 9.

ACKNOWLEDGEMENT

Y.-A.C wants to thank Zhang Jiang for the discussions that inspired the main idea of this paper. Y.-A.C is also grateful to Nat Tantivasadakarn for teaching the polynomial method and its application to the 2d bosonization. We also offer our thanks to Victor Albert, Riley Chien, Daniel Gottesman, Michael Gullans, Mohammad Hafezi, and Ben Reichardt for engaging in very useful discussions with us.

Y.-A.C. is supported by the JQI fellowship. A.V.G. acknowledges funding by NSF QLCI (award No. OMA-2120757), DoE ASCR Accelerated Research

¹¹ The stabilizer G can be added to any term.

in Quantum Computing program (award No. DE-SC0020312), DoE QSA, the DoE ASCR Quantum Testbed Pathfinder program (award No. DE-SC0019040), NSF PFCQC program, AFOSR, ARO MURI, AFOSR MURI, and DARPA SAVANT ADVENT. Y.X. is supported by ARO W911NF-15-1-0397, National Science Foundation QLCI grant OMA-2120757, AFOSR-MURI FA9550-19-1-0399, Department of Energy QSA program. This work is supported by the Laboratory for Physical Sciences through the Condensed Matter Theory Center.

Note added.—As this work was being completed, we also became aware of an independent work, Ref. [29], using a similar polynomial technique to study fermionic quantum simulation from a different perspective.

Appendix A: Syndrome-matching method for finding code distances

In this section, we present an algorithm to find the code distance for a given stabilizer code. We call it the “syndrome matching” method. Specifically, given an integer n , we describe an algorithm to determine whether $d > n$. The algorithm is described as follows.

1. We first choose once vertex to be the origin $(0, 0)$. We then apply a single Pauli from $X_1, Y_1, Z_1, X_2, Y_2, Z_2$ (acting on qubits located on edges $(0, 0) \rightarrow (1, 0)$ and $(0, 0) \rightarrow (0, 1)$). We have 6 cases each of which has its own syndrome vertices, i.e., a set of vertices v that violate the stabilizer G_v . For a single-qubit error, the syndrome set is an ordered set $V^{(1)} = \{(x_1^{(1)}, y_1^{(1)}), (x_2^{(1)}, y_2^{(1)}), \dots\}$, ordered by $x_i^{(1)}: x_1^{(1)} \leq x_2^{(1)} \leq \dots$. If two vertices $i, i+1$ have the same $x_i^{(1)} = x_{i+1}^{(1)}$, they are ordered by $y_i^{(1)} < y_{i+1}^{(1)}$.
2. Ensure that the operator is logical. For this to be the case, all syndrome vertices should vanish. Therefore, we select the first syndrome vertex $(x_1^{(k)}, y_1^{(k)}) \in V^{(k)}$. Then we enumerate all choices of a Pauli matrix on an edge different from the Pauli matrix selected in the previous step(s), such that it cancels the syndrome at $(x_1^{(k)}, y_1^{(k)})$. This operation may generate other syndrome vertices. The syndrome vertices $V^{(k)}$ are updated due to this new Pauli matrix. At this stage, the operator has one more Pauli matrix, and a new ordered set for the syndrome vertices $V^{(k+1)}$. If the syndrome set $V^{(k+1)}$ is empty, this operator is logical. If the operator does not belong to the stabilizer group¹²,

this means that we have found the nontrivial logical operator with the minimum weight. This minimum weight is the code distance and, therefore, we stop the algorithm. Otherwise, we continue.

3. Repeat steps 1 and 2 until the algorithm stops automatically or all cases with operators containing n Pauli matrices have been considered, i.e., all $V^{(n)}$ are checked. If the algorithm stops automatically, it will return the value of the code distance. If the algorithm stops by considering all the cases with n Pauli matrices, we conclude that code distance $d > n$.

Appendix B: 16 elementary automorphisms

In this section, we demonstrate the transformation rules of Pauli matrices for automorphisms A_1, \dots, A_{16} . These automorphisms correspond to applying nearest-neighbor two-qubit Clifford gates.

$$A_1 = \begin{bmatrix} 1 & 0 & | & 0 & 0 \\ 0 & 1 & | & 0 & 0 \\ 0 & 1 & | & 1 & 0 \\ 1 & 0 & | & 0 & 1 \end{bmatrix}, \quad A_2 = \begin{bmatrix} 1 & 0 & | & 0 & 0 \\ 0 & 1 & | & 0 & 0 \\ 0 & y & | & 1 & 0 \\ \bar{y} & 0 & | & 0 & 1 \end{bmatrix}, \quad (\text{B1})$$

$$A_3 = \begin{bmatrix} 1 & 0 & | & 0 & 0 \\ 0 & 1 & | & 0 & 0 \\ 0 & \bar{x} & | & 1 & 0 \\ x & 0 & | & 0 & 1 \end{bmatrix}, \quad A_4 = \begin{bmatrix} 1 & 0 & | & 0 & 0 \\ 0 & 1 & | & 0 & 0 \\ 0 & \bar{x}y & | & 1 & 0 \\ x\bar{y} & 0 & | & 0 & 1 \end{bmatrix}, \quad (\text{B2})$$

$$A_5 = \begin{bmatrix} 1 & 0 & | & 0 & \bar{x}y \\ 0 & 1 & | & x\bar{y} & 0 \\ 0 & 0 & | & 1 & 0 \\ 0 & 0 & | & 0 & 1 \end{bmatrix}, \quad A_6 = \begin{bmatrix} 1 & 0 & | & 0 & y \\ 0 & 1 & | & \bar{y} & 0 \\ 0 & 0 & | & 1 & 0 \\ 0 & 0 & | & 0 & 1 \end{bmatrix}, \quad (\text{B3})$$

$$A_7 = \begin{bmatrix} 1 & 0 & | & 0 & 1 \\ 0 & 1 & | & 1 & 0 \\ 0 & 0 & | & 1 & 0 \\ 0 & 0 & | & 0 & 1 \end{bmatrix}, \quad A_8 = \begin{bmatrix} 1 & 0 & | & 0 & \bar{x} \\ 0 & 1 & | & x & 0 \\ 0 & 0 & | & 1 & 0 \\ 0 & 0 & | & 0 & 1 \end{bmatrix}, \quad (\text{B4})$$

¹² A way to check if a Pauli string operator O belongs to the stabilizer group is by computing $O \cdot (AW)$ and $O \cdot (AU_{1,2})$, where AW and $AU_{1,2}$ generate the full logical space since W and $U_{1,2}$ are the original generators in the exact bosonization and we apply

an automorphism A on them. $O \cdot (AW) = O \cdot (AU_{1,2}) = 0$ if and only if the operator O commutes with all logical operators, which means $O \in \mathcal{G}$ (\mathcal{G} is the stabilizer group).

$$A_9 = \left[\begin{array}{cc|cc} 1 & 0 & 0 & 0 \\ 1 & 1 & 0 & 0 \\ \hline 0 & 0 & 1 & 1 \\ 0 & 0 & 0 & 1 \end{array} \right], \quad A_{10} = \left[\begin{array}{cc|cc} 1 & 0 & 0 & 0 \\ x & 1 & 0 & 0 \\ \hline 0 & 0 & 1 & \bar{x} \\ 0 & 0 & 0 & 1 \end{array} \right], \quad (\text{B5})$$

$$A_{11} = \left[\begin{array}{cc|cc} 1 & 0 & 0 & 0 \\ \bar{y} & 1 & 0 & 0 \\ \hline 0 & 0 & 1 & y \\ 0 & 0 & 0 & 1 \end{array} \right], \quad A_{12} = \left[\begin{array}{cc|cc} 1 & 0 & 0 & 0 \\ x\bar{y} & 1 & 0 & 0 \\ \hline 0 & 0 & 1 & \bar{x}y \\ 0 & 0 & 0 & 1 \end{array} \right], \quad (\text{B6})$$

$$A_{13} = \left[\begin{array}{cc|cc} 1 & 1 & 0 & 0 \\ 0 & 1 & 0 & 0 \\ \hline 0 & 0 & 1 & 0 \\ 0 & 0 & 1 & 1 \end{array} \right], \quad A_{14} = \left[\begin{array}{cc|cc} 1 & \bar{x} & 0 & 0 \\ 0 & 1 & 0 & 0 \\ \hline 0 & 0 & 1 & 0 \\ 0 & 0 & x & 1 \end{array} \right], \quad (\text{B7})$$

$$A_{15} = \left[\begin{array}{cc|cc} 1 & y & 0 & 0 \\ 0 & 1 & 0 & 0 \\ \hline 0 & 0 & 1 & 0 \\ 0 & 0 & \bar{y} & 1 \end{array} \right], \quad A_{16} = \left[\begin{array}{cc|cc} 1 & \bar{x}y & 0 & 0 \\ 0 & 1 & 0 & 0 \\ \hline 0 & 0 & 1 & 0 \\ 0 & 0 & x\bar{y} & 1 \end{array} \right]. \quad (\text{B8})$$

The diagonal blocks of A_1 are identities, and its nontrivial part is the lower left block which attaches an extra Z to X_1 and X_2 . By multiplying the polynomial vectors of X_1 , X_2 , Z_1 , and Z_2 by automorphism A_1 , we get the following terms:

$$\begin{aligned} -X_e- & \xrightarrow{A_1} \begin{array}{c} | \\ Z \\ | \\ -X_e- \end{array}, \\ \begin{array}{c} | \\ X_e \\ | \end{array} & \xrightarrow{A_1} \begin{array}{c} | \\ X_e \\ | \\ -Z- \end{array}, \\ -Z_e- & \xrightarrow{A_1} -Z_e-, \\ \begin{array}{c} | \\ Z_e \\ | \end{array} & \xrightarrow{A_1} \begin{array}{c} | \\ Z_e \\ | \end{array}. \end{aligned} \quad (\text{B9})$$

Similarly, we may multiply X_1 , X_2 , Z_1 , and Z_2 by A_2 , thereby obtaining

$$\begin{aligned} -X_e- & \xrightarrow{A_2} \begin{array}{c} | \\ -X_e- \\ | \\ Z \\ | \end{array}, \\ \begin{array}{c} | \\ X_e \\ | \end{array} & \xrightarrow{A_2} \begin{array}{c} | \\ -Z- \\ | \\ X_e \\ | \end{array}, \\ -Z_e- & \xrightarrow{A_2} -Z_e-, \\ \begin{array}{c} | \\ Z_e \\ | \end{array} & \xrightarrow{A_2} \begin{array}{c} | \\ Z_e \\ | \end{array}. \end{aligned} \quad (\text{B10})$$

Following the same argument, we can obtain pictorial representations for the rest of the automorphisms.

A_3 :

$$\begin{aligned} -X_e- & \xrightarrow{A_3} \begin{array}{c} | \\ Z \\ | \\ -X_e- \end{array}, \\ \begin{array}{c} | \\ X_e \\ | \end{array} & \xrightarrow{A_3} \begin{array}{c} | \\ X_e \\ | \\ -Z- \end{array}, \\ -Z_e- & \xrightarrow{A_3} -Z_e-, \\ \begin{array}{c} | \\ Z_e \\ | \end{array} & \xrightarrow{A_3} \begin{array}{c} | \\ Z_e \\ | \end{array}. \end{aligned} \quad (\text{B11})$$

A_4 :

$$\begin{aligned} -X_e- & \xrightarrow{A_4} \begin{array}{c} | \\ -X_e- \\ | \\ Z \\ | \end{array}, \\ \begin{array}{c} | \\ X_e \\ | \end{array} & \xrightarrow{A_4} \begin{array}{c} | \\ -Z- \\ | \\ X_e \\ | \end{array}, \\ -Z_e- & \xrightarrow{A_4} -Z_e-, \\ \begin{array}{c} | \\ Z_e \\ | \end{array} & \xrightarrow{A_4} \begin{array}{c} | \\ Z_e \\ | \end{array}. \end{aligned} \quad (\text{B12})$$

$A_5:$

$$\begin{array}{ccc}
-X_e- & \xrightarrow{A_5} & -X_e- \\
\downarrow & & \downarrow \\
X_e & \xrightarrow{A_5} & X_e \\
\downarrow & & \downarrow \\
-Z_e- & \xrightarrow{A_5} & \begin{array}{c} -Z_e- \\ | \\ X \end{array} \\
\downarrow & & \downarrow \\
Z_e & \xrightarrow{A_5} & \begin{array}{c} -X- \\ | \\ Z_e \end{array}
\end{array} \quad (B13)$$

 $A_8:$

$$\begin{array}{ccc}
-X_e- & \xrightarrow{A_8} & -X_e- \\
\downarrow & & \downarrow \\
X_e & \xrightarrow{A_8} & X_e \\
\downarrow & & \downarrow \\
-Z_e- & \xrightarrow{A_8} & \begin{array}{c} | \\ X \\ | \\ -Z_e- \end{array} \\
\downarrow & & \downarrow \\
Z_e & \xrightarrow{A_8} & \begin{array}{c} | \\ Z_e \\ | \\ -X- \end{array}
\end{array} \quad (B16)$$

 $A_6:$

$$\begin{array}{ccc}
-X_e- & \xrightarrow{A_6} & -X_e- \\
\downarrow & & \downarrow \\
X_e & \xrightarrow{A_6} & X_e \\
\downarrow & & \downarrow \\
-Z_e- & \xrightarrow{A_6} & \begin{array}{c} -Z_e- \\ | \\ X \end{array} \\
\downarrow & & \downarrow \\
Z_e & \xrightarrow{A_6} & \begin{array}{c} -X- \\ | \\ Z_e \end{array}
\end{array} \quad (B14)$$

 $A_9:$

$$\begin{array}{ccc}
-X_e- & \xrightarrow{A_9} & \begin{array}{c} | \\ X \\ | \\ -X_e- \end{array} \\
\downarrow & & \downarrow \\
X_e & \xrightarrow{A_9} & X_e \\
\downarrow & & \downarrow \\
-Z_e- & \xrightarrow{A_9} & -Z_e- \\
\downarrow & & \downarrow \\
Z_e & \xrightarrow{A_9} & \begin{array}{c} | \\ Z_e \\ | \\ -Z- \end{array}
\end{array} \quad (B17)$$

 $A_7:$

$$\begin{array}{ccc}
-X_e- & \xrightarrow{A_7} & -X_e- \\
\downarrow & & \downarrow \\
X_e & \xrightarrow{A_7} & X_e \\
\downarrow & & \downarrow \\
-Z_e- & \xrightarrow{A_7} & \begin{array}{c} | \\ X \\ | \\ -Z_e- \end{array} \\
\downarrow & & \downarrow \\
Z_e & \xrightarrow{A_7} & \begin{array}{c} | \\ Z_e \\ | \\ -X- \end{array}
\end{array} \quad (B15)$$

 $A_{10}:$

$$\begin{array}{ccc}
-X_e- & \xrightarrow{A_{10}} & \begin{array}{c} | \\ X \\ | \\ -X_e- \end{array} \\
\downarrow & & \downarrow \\
X_e & \xrightarrow{A_{10}} & X_e \\
\downarrow & & \downarrow \\
-Z_e- & \xrightarrow{A_{10}} & -Z_e- \\
\downarrow & & \downarrow \\
Z_e & \xrightarrow{A_{10}} & \begin{array}{c} | \\ Z_e \\ | \\ -Z- \end{array}
\end{array} \quad (B18)$$

A_{11} :

$$\begin{array}{ccc}
-X_e- & \xrightarrow{A_{11}} & \begin{array}{c} -X_e- \\ | \\ X \\ | \end{array} \\
| & & \\
X_e & \xrightarrow{A_{11}} & X_e \\
| & & | \\
-Z_e- & \xrightarrow{A_{11}} & -Z_e- \\
| & & \\
Z_e & \xrightarrow{A_{11}} & \begin{array}{c} -Z- \\ | \\ Z_e \\ | \end{array}
\end{array} \quad (B19)$$

 A_{12} :

$$\begin{array}{ccc}
-X_e- & \xrightarrow{A_{12}} & \begin{array}{c} -X_e- \\ | \\ X \\ | \end{array} \\
| & & \\
X_e & \xrightarrow{A_{12}} & X_e \\
| & & | \\
-Z_e- & \xrightarrow{A_{12}} & -Z_e- \\
| & & \\
Z_e & \xrightarrow{A_{12}} & \begin{array}{c} -Z- \\ | \\ Z_e \\ | \end{array}
\end{array} \quad (B20)$$

 A_{13} :

$$\begin{array}{ccc}
-X_e- & \xrightarrow{A_{13}} & -X_e- \\
| & & \\
X_e & \xrightarrow{A_{13}} & \begin{array}{c} X_e \\ | \\ -X- \end{array} \\
| & & \\
-Z_e- & \xrightarrow{A_{13}} & \begin{array}{c} | \\ Z \\ | \\ -Z_e- \end{array} \\
| & & \\
Z_e & \xrightarrow{A_{13}} & Z_e
\end{array} \quad (B21)$$

 A_{14} :

$$\begin{array}{ccc}
-X_e- & \xrightarrow{A_{14}} & -X_e- \\
| & & \\
X_e & \xrightarrow{A_{14}} & \begin{array}{c} X_e \\ | \\ -X- \\ | \\ X_e \end{array} \\
| & & \\
-Z_e- & \xrightarrow{A_{14}} & \begin{array}{c} -Z_e- \\ | \\ Z \\ | \\ -Z_e- \end{array} \\
| & & \\
Z_e & \xrightarrow{A_{14}} & Z_e
\end{array} \quad (B22)$$

 A_{15} :

$$\begin{array}{ccc}
-X_e- & \xrightarrow{A_{15}} & -X_e- \\
| & & \\
X_e & \xrightarrow{A_{15}} & \begin{array}{c} -X- \\ | \\ X_e \\ | \\ -Z_e- \end{array} \\
| & & \\
-Z_e- & \xrightarrow{A_{15}} & \begin{array}{c} -Z_e- \\ | \\ Z \\ | \\ -Z_e- \end{array} \\
| & & \\
Z_e & \xrightarrow{A_{15}} & Z_e
\end{array} \quad (B23)$$

 A_{16} :

$$\begin{array}{ccc}
-X_e- & \xrightarrow{A_{16}} & -X_e- \\
| & & \\
X_e & \xrightarrow{A_{16}} & \begin{array}{c} -X- \\ | \\ X_e \\ | \\ -Z_e- \end{array} \\
| & & \\
-Z_e- & \xrightarrow{A_{16}} & \begin{array}{c} -Z_e- \\ | \\ Z \\ | \\ -Z_e- \end{array} \\
| & & \\
Z_e & \xrightarrow{A_{16}} & Z_e
\end{array} \quad (B24)$$

Appendix C: Automorphisms for code distances $d = 6$ and $d = 7$

In this section, we show the explicit form of automorphisms $A^{d=6}$ and $A^{d=7}$ found by syndrome matching. The automorphism $A^{d=6} = A_1 A_5 A_{14} A_1$ has a code dis-

tance of 6:

$$A^{d=6} = \left[\begin{array}{cc|cc} 1 + \bar{x}y & \bar{x} + y & y & \bar{x}y \\ 0 & 1 + x\bar{y} & x\bar{y} & 0 \\ 0 & x\bar{y} & 1 + x\bar{y} & 0 \\ \bar{x}y & \bar{x} + x + y & x + y & 1 + \bar{x}y \end{array} \right]. \quad (\text{C1})$$

By applying $A^{d=6}$ on logical operators U_1 , U_2 , W , and stabilizer G , we obtain their polynomial representations

as follows:

$$A^{d=6}U_1 = \left[\begin{array}{c} \bar{x} + 1 + \bar{x}y \\ 0 \\ 0 \\ \bar{y} + \bar{x} + \bar{x}y \end{array} \right], \quad (\text{C2})$$

$$A^{d=6}U_2 = \left[\begin{array}{c} \bar{x} + \bar{x}y + y \\ \bar{y} + x\bar{y} + 1 \\ \bar{y} + x\bar{y} + \bar{x} \\ \bar{x} + 1 + x + \bar{x}y + y \end{array} \right], \quad (\text{C3})$$

$$A^{d=6}W = \left[\begin{array}{c} \bar{x}y + y^2 \\ x\bar{y} + x \\ x\bar{y} + 1 + x + y \\ 1 + \bar{x}y + xy + y^2 \end{array} \right], \quad (\text{C4})$$

$$A^{d=6}G = \left[\begin{array}{c} \bar{x}\bar{y} + \bar{x}^2y + y + y^2 \\ x\bar{y}^2 + \bar{y} + 1 + x \\ x\bar{y}^2 + 1 + x + y \\ \bar{x}\bar{y} + x\bar{y} + \bar{x} + x + \bar{x}^2y + y + xy + y^2 \end{array} \right]. \quad (\text{C5})$$

The automorphism $A^{d=7} = A_1A_{11}A_5A_{14}A_9$ with distance $d = 7$ is

$$A^{d=7} = \left[\begin{array}{cc|cc} \bar{x} + 1 & \bar{x} & y & \bar{x}y + y \\ \bar{x}\bar{y} + \bar{y} + 1 & \bar{x}\bar{y} + 1 & x\bar{y} + 1 & x\bar{y} + \bar{x} + 1 \\ \bar{x}\bar{y} + \bar{y} + 1 & \bar{x}\bar{y} + 1 & x\bar{y} + xy & x\bar{y} + \bar{x} + y + xy \\ \bar{x} + 1 & \bar{x} & x + y & 1 + x + \bar{x}y + y \end{array} \right]. \quad (\text{C6})$$

By applying $A^{d=7}$ on logical operators U_1 , U_2 , W , and stabilizer G , we can write down their polynomial representations as follows:

$$A^{d=7}U_1 = \left[\begin{array}{c} 0 \\ x\bar{y}^2 + 1 \\ x\bar{y}^2 + \bar{y} + x \\ \bar{y} + x\bar{y} \end{array} \right], \quad A^{d=7}U_2 = \left[\begin{array}{c} \bar{x} + \bar{x}y \\ \bar{x}\bar{y} + \bar{y} + \bar{x} + 1 \\ \bar{x}\bar{y} + \bar{y} + 1 + y \\ \bar{x} + 1 + \bar{x}y \end{array} \right], \quad (\text{C7})$$

$$A^{d=7}W = \left[\begin{array}{c} \bar{x}y + y + xy + y^2 \\ x^2\bar{y} + \bar{x} + 1 + y \\ x^2\bar{y} + \bar{x} + 1 + x + y + xy + x^2y + xy^2 \\ 1 + x + x^2 + \bar{x}y + y + y^2 \end{array} \right], \quad (\text{C8})$$

$$A^{d=7}G = \left[\begin{array}{c} \bar{x}\bar{y} + \bar{x}^2 + \bar{x} + 1 + \bar{x}y + y + xy + xy^2 \\ \bar{x}y^2 + \bar{x}^2\bar{y} + \bar{x}\bar{y} + x\bar{y} + 1 + y \\ \bar{x}y^2 + \bar{x}^2\bar{y} + \bar{x}\bar{y} + x^2\bar{y} \\ + 1 + x + y + xy + x^2y + xy^2 \\ \bar{x}\bar{y} + \bar{x}^2 + \bar{x} + x + x^2 + \bar{x}y + y + y^2 \end{array} \right]. \quad (\text{C9})$$

-
- [1] Daniel Gottesman, *Stabilizer codes and quantum error correction* (California Institute of Technology, 1997).
- [2] Sergey B. Bravyi and Alexei Yu. Kitaev, “Fermionic quantum computation,” *Annals of Physics* **298**, 210 – 226 (2002).
- [3] Frank Arute, Kunal Arya, Ryan Babbush, Dave Bacon, Joseph C Bardin, Rami Barends, Andreas Bengtsson, Sergio Boixo, Michael Broughton, Bob B Buckley, *et al.*, “Observation of separated dynamics of charge and spin in the fermi-hubbard model,” arXiv preprint arXiv:2010.07965 (2020).
- [4] A.Yu. Kitaev, “Fault-tolerant quantum computation by anyons,” *Annals of Physics* **303**, 2–30 (2003).
- [5] Austin G. Fowler, Matteo Mariantoni, John M. Martinis, and Andrew N. Cleland, “Surface codes: Towards practical large-scale quantum computation,” *Phys. Rev. A* **86**, 032324 (2012).
- [6] Kanav Setia, Sergey Bravyi, Antonio Mezzacapo, and James D. Whitfield, “Superfast encodings for fermionic quantum simulation,” *Phys. Rev. Research* **1**, 033033 (2019).
- [7] R. C. Ball, “Fermions without fermion fields,” *Phys. Rev. Lett.* **95**, 176407 (2005).
- [8] F Verstraete and J I Cirac, “Mapping local hamiltonians of fermions to local hamiltonians of spins,” *Journal of Statistical Mechanics: Theory and Experiment* **2005**, P09012–P09012 (2005).
- [9] James D. Whitfield, Vojtěch Havlíček, and Matthias Troyer, “Local spin operators for fermion simulations,” *Phys. Rev. A* **94**, 030301 (2016).
- [10] Mark Steudtner and Stephanie Wehner, “Quantum codes for quantum simulation of fermions on a square lattice of qubits,” *Phys. Rev. A* **99**, 022308 (2019).
- [11] Charles Derby, Joel Klassen, Johannes Bausch, and Toby Cubitt, “Compact fermion to qubit mappings,” *Phys. Rev. B* **104**, 035118 (2021).
- [12] Hoi Chun Po, “Symmetric jordan-wigner transformation in higher dimensions,” arXiv preprint arXiv:2107.10842 (2021).
- [13] Yu-An Chen, Anton Kapustin, and Djordje Radicevic, “Exact bosonization in two spatial dimensions and a new class of lattice gauge theories,” *Annals of Physics* **393**, 234 – 253 (2018).
- [14] Yu-An Chen and Anton Kapustin, “Bosonization in three spatial dimensions and a 2-form gauge theory,” *Phys. Rev. B* **100**, 245127 (2019).
- [15] Yu-An Chen, “Exact bosonization in arbitrary dimensions,” *Phys. Rev. Research* **2**, 033527 (2020).
- [16] Arkadiusz Bochniak, Błażej Ruba, Jacek Wosiek, and Adam Wyrzykowski, “Constraints of kinematic bosonization in two and higher dimensions,” *Physical Review D* **102**, 114502 (2020).
- [17] Arkadiusz Bochniak and Błażej Ruba, “Bosonization based on clifford algebras and its gauge theoretic interpretation,” *Journal of High Energy Physics* **2020**, 1–36 (2020).
- [18] Arkadiusz Bochniak, Błażej Ruba, and Jacek Wosiek, “Bosonization of majorana modes and edge states,” *Physical Review B* **105**, 155105 (2022).
- [19] Mark Steudtner and Stephanie Wehner, “Fermion-to-qubit mappings with varying resource requirements for quantum simulation,” *New Journal of Physics* **20**, 063010 (2018).
- [20] Riley W Chien and James D Whitfield, “Custom fermionic codes for quantum simulation,” arXiv preprint arXiv:2009.11860 (2020).
- [21] Yu-An Chen and Yijia Xu, “Equivalence between fermion-to-qubit mappings in two spatial dimensions,” (2022).
- [22] Abhishek Rajput, Alessandro Roggero, and Nathan Wiebe, “Quantum error correction with gauge symmetries,” arXiv preprint arXiv:2112.05186 (2021).
- [23] Zhang Jiang, Jarrod McClean, Ryan Babbush, and Hartmut Neven, “Majorana loop stabilizer codes for error mitigation in fermionic quantum simulations,” *Phys. Rev. Applied* **12**, 064041 (2019).
- [24] Jeongwan Haah, “Commuting pauli hamiltonians as maps between free modules,” *Communications in Mathematical Physics* **324**, 351–399 (2013).
- [25] Jeongwan Haah, “Algebraic methods for quantum codes on lattices,” *Revista Colombiana de Matemáticas* **50**, 299–349 (2016).
- [26] Błażej Ruba and Bowen Yang, “Homological invariants of pauli stabilizer codes,” (2022).
- [27] Nathanan Tantivasadakarn, “Jordan-wigner dualities for translation-invariant hamiltonians in any dimension: Emergent fermions in fracton topological order,” *Phys. Rev. Research* **2**, 023353 (2020).
- [28] Jeongwan Haah, “Clifford quantum cellular automata: Trivial group in 2d and witt group in 3d,” *Journal of Mathematical Physics* **62**, 092202 (2021), <https://doi.org/10.1063/5.0022185>.
- [29] Riley W. Chien and Joel Klassen, “Optimizing fermionic encodings for both hamiltonian and hardware,” (2022), arXiv:2210.05652 [quant-ph].